

Impact of correlations and finite temperatures on the anomalous Hall conductivity of 3d-transition-metals

Diemo Ködderitzsch,^{1,*} Kristina Chadova,¹ Ján Minár,¹ and Hubert Ebert¹

¹*Department Chemie, Physikalische Chemie, Universität München, Butenandstr. 5-13, 81377 München, Germany*
(ΩDated: February 5, 2018)

Employing the linear response Kubo formalism as implemented in a fully relativistic multiple-scattering Korringa-Kohn-Rostoker Green function method a systematic first-principles study based on density-functional theory (DFT) of the anomalous Hall conductivity (AHC) of the 3d-transition-metals Fe, Co and Ni is presented. To account for the temperature dependence of the AHC an alloy-analogy for a set of thermal lattice displacements acting as a scattering mechanism is used which is subsequently solved using the coherent potential approximation. Further, impurity scattering has been considered to elucidate the importance of an additional possible contribution to the AHC that might be present in experiment. The impact of correlations beyond the local spin-density approximation to the exchange-correlation functional in DFT is studied within the LSDA+*U* approach. It is shown that both, the inclusion of correlations and thermal lattice vibrations, is needed to give a material-specific description of the AHC in transition-metals.

PACS numbers: 71.15.Mb,71.15.Rf,72.15.-v,72.25.Ba,75.76.+j,85.75.-d

The simple experiment by Hall [1] driving a current through a ferromagnet and observing the anomalous Hall effect (AHE) as a transverse voltage has fruitfully spurred the development of experimental and theoretical methods dealing with transport in solids. It now stands as a paradigm for understanding related transverse transport phenomena, like e. g. the spin Hall- (SHE), anomalous- and Spin-Nernst effect which have received intense interest in recent years. They all share a common origin, namely they are manifestly spin-orbit driven *relativistic* effects.

The AHE has for decades eluded theoretical understanding – it took more than 50 years until Karplus and Luttinger [2] put forward an insight which initiated modern theories of the AHE. They identified the anomalous velocity as an interband matrix element of the current operator which is nowadays the foundation of semiclassical approaches which give a topological formulation of the AHE in terms of the Berry phase of Bloch bands in pure crystals [3, 4]. The latter is used to define the so called intrinsic contribution to the AHE. Already early on Smit [5] and Berger [6] discussed other extrinsic origins of the AHE, namely skew- and side-jump scattering. There are contributions to the AHE which fall in neither category, [4] while it is now commonly established to separate the AHE into an intrinsic and a skew-scattering contribution and declare the difference to the total AHE as side-jump [7]. Experiments then rely on scaling mechanism to extract these contributions from the raw data.

Besides a wealth of model calculations (see the review [7] and references therein) which are tailored to identify general trends but miss the material specific aspect a number of first-principles calculations building on a density-functional theory (DFT) framework employing the local spin density (LSDA) or generalized gradient (GGA) approximations have been undertaken recently

to compute the anomalous Hall conductivity (AHC) in the transition-metals (TM) [8–10]. Almost all of them rely on the Berry phase formulation for pure crystals and therefore are only able to deal with the intrinsic contribution. Boltzmann-transport theory based formulations have been used in the context of the SHE [11] to compute the skew-scattering contributions in the dilute limit for alloys. Covering the whole concentration range of alloys and including all contributions to the AHE has recently been done [12, 13] on the basis of a Kubo-Středa formulation [14, 15].

The role of correlations in the electronic structure of the 3d-TM has only very recently been addressed in the context of the AHE [9, 10]. Employing the LSDA turns out to give unfavorable agreement with experiment, and with the AHE being a property of the Fermi-surface [8, 16] it became clear that the LSDA does not supply the proper bandstructure. This is demonstrated in particular for the case of Ni (see also table I) where the LSDA/GGA strongly overestimates the magnitude of the AHC. Employing the LSDA/GGA+*U* remedies this problem, by moving down *d*-bands relative to the Fermi-energy (E_F), thereby making the X_2 hole pocket present in LSDA/GGA disappear.

A further important aspect of the AHE which is addressed in experimental studies but rarely in theoretical considerations is the temperature dependence of the AHE. For the pure 3d-systems measurements of the AHE are typically done on commercially available specimen or thick layers grown on a substrate [17–19] and the temperature is changed in order to vary the resistivity. The latter makes the discussion of the temperature dependence very delicate when trying to disentangle different mechanisms and contributions to the AHE (inelastic scattering, scattering by phonons/magnons, etc.). It is advocated, however, as an *empirical fact* [7, 20] that inelastic scat-

tering processes suppress the skew-scattering at higher temperatures with the intrinsic and side-jump (see however remark above) contributions dominantly prevailing. This then again is used to experimentally analyze the AHE. Recently model calculations [20] studied the role of inelastic scattering by phonons employing a Kubo-formalism and introducing a phenomenological scattering rate γ as the imaginary part of the self-energy. To our knowledge no first-principles approach has been used so far to deal with the temperature dependence of AHE in 3d-TM.

In this letter we present a generally applicable formalism and results of a first-principles approach for calculating the anomalous Hall conductivity of transition metals and their alloys. We show that the inclusion of both finite temperature *and* correlation effects leads to a unified material specific description of these systems.

As the AHE is inherently a relativistic phenomenon we choose to work within a fully relativistic approach employing the Kohn-Sham-Dirac equation as formulated in spin-polarized-DFT employing the Hamiltonian:

$$\mathcal{H}_D = -ic\vec{\alpha} \cdot \vec{\nabla} + mc^2\beta + \bar{V}_{KS}(\vec{r}) + \beta\vec{\Sigma} \cdot \vec{B}_{xc}(\vec{r}), \quad (1)$$

with \bar{V}_{KS} and \vec{B}_{xc} being the spin-averaged and spin-dependent part of the one-particle potential, respectively, and the relativistic matrices $\vec{\alpha}$, β and $\vec{\Sigma}$ having the usual meaning [21–23]. This has the important advantage [15] that disorder can be treated elegantly without making recourse to a Pauli approach which poses difficulties in calculating the vertex corrections. To determine longitudinal and transverse components of the conductivity tensor a natural starting point is the linear response Kubo framework which also can be used to derive the Berry phase related semiclassical approach [3, 4, 24]. The Kubo approach has important advantages as compared to the latter. It allows straight-forwardly to include disorder, therefore not only being able to describe pure systems, but also alloys of the full concentration range including intrinsic and extrinsic contributions to the AHE [12, 13]. Further making use of an alloy analogy model (see below) finite temperatures can be accounted for. It also allows to include correlations beyond LSDA in the framework of LSDA+ U or LSDA+DMFT [25, 26]. For cubic and hexagonal systems with the magnetization pointing along the \hat{e}_z -direction, the AHE is given [14, 15] by the off-diagonal tensor element $\sigma_{yx} = -\sigma_{xy}$ of:

$$\begin{aligned} \sigma_{\mu\nu} = & \frac{\hbar}{4\pi N\Omega} \text{Trace} \langle \hat{j}_\mu (G^+ - G^-) \hat{j}_\nu G^- \\ & - \hat{j}_\mu G^+ \hat{j}_\nu (G^+ - G^-) \rangle_c \\ & + \frac{|e|}{4\pi i N\Omega} \text{Trace} \langle (G^+ - G^-) (\hat{r}_\mu \hat{j}_\nu - \hat{r}_\nu \hat{j}_\mu) \rangle_c, \end{aligned} \quad (2)$$

with the relativistic current operator $\hat{j} = -|e|c\vec{\alpha}$ and the electronic retarded and advanced Green functions G^\pm which in the framework of the presented KKR approach

are given in a relativistic multiple scattering representation [27]. The angular brackets denote a configurational average which here is carried out using the coherent potential approximation (CPA) which allows to include vertex corrections (vc), which are of utter importance for the *quantitative* determination of both the longitudinal and transversal conductivity in alloys. As has been argued and also shown [7, 12, 13] calculations omitting the vc's give the intrinsic AHC. Thereby, subtracting the latter from the AHC obtained from the value including the vc's the extrinsic part can be extracted.

Several sources of electron scattering at finite temperatures will determine the T -dependence of the AHE. We neglect the redistribution of states due to finite temperature in the electronic subsystem as well as electron-magnon interaction and consider as a dominant effect only thermal lattice vibrations. To include the latter as a source of electron scattering one could generalize Eq. (2) to finite temperatures by including the electron-phonon self-energy $\Sigma_{\text{el-ph}}$ when calculating the Greens function G^\pm . This, however, is computationally very expensive. Therefore the consideration is restricted to elastic scattering processes by using a quasi-static representation of the thermal displacements of the atoms from their equilibrium positions as has already been used successfully by the authors in the theory of Gilbert-damping [28]. Treating each displaced atom as an alloy partner, we introduce an alloy-analogy model to average over a discrete set of displacements that is chosen to reproduce the thermal root mean square average displacement $\sqrt{\langle u^2 \rangle_T}$ for a given temperature T . This was chosen according to $\langle u^2 \rangle_T = \frac{1}{4} \frac{3h^2}{\pi^2 mk \Theta_D} [\frac{\Phi(\Theta_D/T)}{\Theta_D/T} + \frac{1}{4}]$ with $\Phi(\Theta_D/T)$ the Debye function, h the Planck constant, k the Boltzmann constant and Θ_D the Debye temperature [29]. Ignoring the zero temperature term $1/4$ and assuming a frozen potential for the atoms, the situation can be dealt with in full analogy to the treatment of disordered alloys described above. To assess the presented approach the diagonal resistivities (i. e. ρ_{xx}) were calculated for the 3d-TM making use of the Kubo-Greenwood expression for the symmetric part of the conductivity tensor [30–32]. The results are shown as insets in Figs. 2 and 3 and compared with experimental data taken from the literature. As can be seen the agreement is rather good. Therefore we expect the aforementioned framework to be a reasonable approximation to properly describe electron-phonon scattering and the temperature dependence of the AHE.

To study the impact of correlations (beyond LSDA) LSDA+ U [36] calculations have been performed keeping $J_{\text{eff}} = 0.9\text{eV}$ fixed and scanning the U -range up to typical values employed for the 3d-TMs. In Fig. 1 the dependence of the intrinsic AHE at $T = 0\text{K}$ for bcc-Fe, hcp-Co and fcc-Ni is shown. Whereas for Fe and Co only small variations of the AHC are observed, a pronounced U -dependence for Ni is seen with the experimentally ex-

TABLE I. The intrinsic AHC σ_{yx} in $(\Omega\text{cm})^{-1}$ of the ferromagnetic transition metals Fe, Co and Ni from *first-principles* theoretical (present work compared to other) as well as experimental (Exp.) studies. The magnetization has been assumed to be oriented along the [001] direction.

	bcc-Fe	hcp-Co	fcc-Co	fcc-Ni
LSDA, present work	685	325	213	-2062
LSDA+ U , present work	703	390	379	-1092
LSDA/GGA	753 ^a , 767 ^b	477 ^a	249 ^c	-2203 ^a , -2200 ^d
	650 ^e	481 ^c	360 ^e	-2410 ^e
LSDA/GGA+ U				-960 ^d , -900 ^b
Exp.	1032 ^f	813		-646(@ RT) ^g -1100(5K) ^h

^a Ref. 8.

^b Ref. 9.

^c Ref. 33.

^d Ref. 10.

^e Ref. 13.

^f Ref. 34.

^g Ref. 35.

^h Ref. 18.

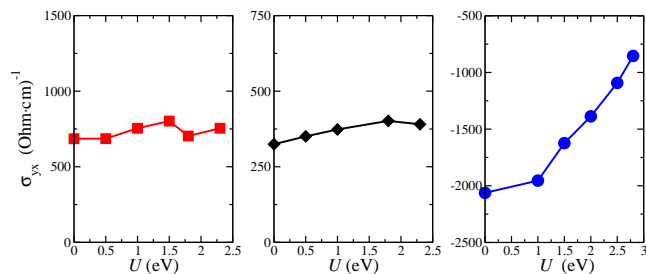


FIG. 1. (Color online) The dependence of the AHC ($T=0$ K) bcc-Fe, hcp-Co and fcc-Ni as a function of the U -value in the LSDA+ U calculation.

tracted intrinsic value of -1100 S/cm recovered at a U -value of around 2.5eV (this value is also used in calculation of the T -dependence below). Analysis shows that this is due to a down shift of minority $3d$ -bands w.r.t. E_F and a vanishing hole pocket at the X_2 point as has already been recently discussed [10]. In table I we show the calculated values for Fe ($U = 1.8\text{eV}$), Co (hcp and fcc, $U = 2.3\text{eV}$) and Ni ($U = 2.5\text{eV}$) [37] in comparison to other calculations as well as experiment.

Early measurements of the AHE in Ni report a value of -646 S/cm at room temperature. [35] Recent experimental work [18] analyzed this in more detail claiming the AHE to consist of an intrinsic component of about -1100 S/cm and a sizable skew-scattering contribution at low temperatures, which both diminish at higher temperatures albeit with different rates. In Fig. 2 the calculated temperature dependence of the AHE in Ni using LSDA and LSDA+ U ($U = 2.5$ eV, $J_{\text{eff}} = 0.9$ eV) as well as experimental results [18] are shown. As could be expected from the above the LSDA result strongly overesti-

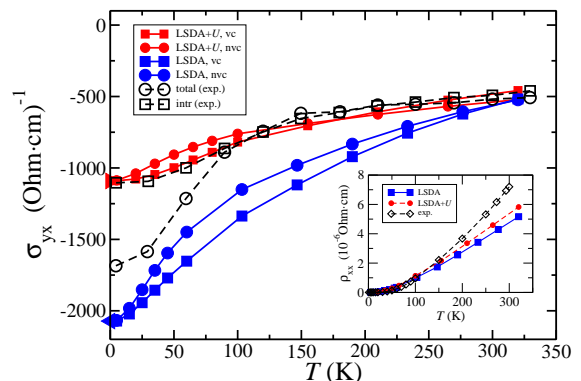


FIG. 2. (Color online) The temperature dependence of the AHC of Ni. Shown are theoretical results obtained by LSDA, LSDA+ U both including (vc) and excluding (nvc) vertex corrections and experimental data [18]. Triangle symbols denote the zero temperature values intrinsic AHE values for LSDA and LSDA+ U , respectively. The inset shows the longitudinal ρ_{xx} component of the resistivity as compared to experiment [38].

mates the magnitude over the whole temperature range, whereas the LSDA+ U fairly well reproduces the experimental result. This demonstrates that both correlations beyond LSDA as well as temperature induced thermal vibrations combined need to be taken into account. The vertex corrections due to the the lattice vibrations have little impact in the low T -regime and are negligible at higher temperatures such that, as seen in experiment, the intrinsic contribution survives. The deviation from the total AHC in the low T -range we attribute to possible impurities that might be present in the sample. In contrast to Ni the temperature dependence in Fe (see Fig. 3)

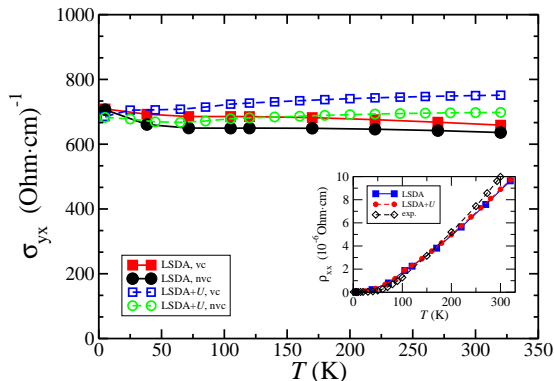


FIG. 3. (Color online) The temperature dependence of the AHC of Fe as calculated in LSDA and LSDA+ U . The insets show the longitudinal ρ_{xx} component of the resistivity as compared to experiment [38].

is found to be small.

In the context of both the SHE and the AHE, [11, 12, 39, 40] it has already been shown that in the dilute/super-clean limit large skew scattering contributions can arise with the AHC scaling as $\sigma_{yx} \propto \sigma_{xx}$. To demonstrate this and put it in the context of the recent experiment by Ye *et al.* [18] we performed calculation for Mg impurities and Fe impurities in Ni. As can be seen in Fig 4 the calculated full AHC (including vc's) approaches the experimental curve for higher temperatures. However in the low temperature regime larger deviations are visible. Taking the difference between the calculation with vc's to those without vc's (intrinsic values), one also observes that the impurity induced extrinsic contribution for Mg shows the same sign as seen in experiment, i. e. it increases the absolute value, whereas for Fe impurities the opposite behavior is seen. This highlights again the fact that the skew-scattering component in an impurity specific way determines the quantitative low temperature behavior of the AHC in clean $3d$ -metals but also that the experimental determination of “clean” systems is extremely challenging.

In summary, we have used the linear response Kubo formalism as implemented in a fully relativistic multiple-scattering KKR Green function method to study systematically from first-principles the anomalous Hall conductivity (AHC) of the $3d$ -transition-metals Fe, Co and Ni. Going beyond the local spin-density approximation in DFT employing the LSDA+ U and including finite temperatures by using a CPA-alloy analogy for the lattice displacements provided the necessary means to allow for a material specific description of the AHC. Further, the impact of dilute impurities has been analyzed. The presented framework is now ready to be applied to the whole concentration range of correlated TM-alloys. Treating correlations beyond the static limit (LSDA+ U) of the LSDA+DMFT combined with a linear response trans-

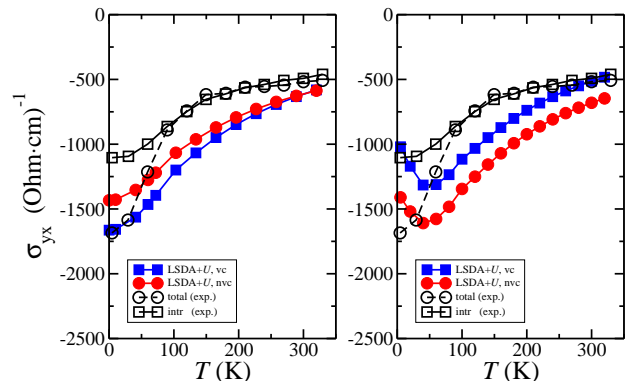


FIG. 4. (Color online) The temperature dependence of the AHC of $\text{Ni}_{0.98}\text{Mg}_{0.02}$ (left) and $\text{Ni}_{0.98}\text{Fe}_{0.02}$ (right) as calculated in LSDA+ U compared to experiment [18].

port formalism is a major issue for future work.

The authors would like to thank the DFG for financial support within the SFB 689, FOR 1346 and SPP 1538. Discussions with Sergei Mankowsky are gratefully acknowledged.

* dkopc@cup.uni-muenchen.de

- [1] E. H. Hall, *Phil. Mag.* **12**, 157 (1881).
- [2] R. Karplus and J. M. Luttinger, *Phys. Rev.* **95**, 1154 (1954).
- [3] T. Jungwirth, Q. Niu, and A. H. MacDonald, *Phys. Rev. Lett.* **88**, 207208 (2002).
- [4] N. A. Sinitsyn, *J. Phys.: Cond. Mat.* **20**, 023201 (2008).
- [5] J. Smit, *Physica* **21**, 877 (1955).
J. Smit, *Physica* **24**, 39 (1958).
- [6] L. Berger, *Phys. Rev. B* **2**, 4559 (1970).
- [7] N. Nagaosa, J. Sinova, S. Onoda, A. H. MacDonald, and N. P. Ong, *Rev. Mod. Phys.* **82**, 1539 (2010).
- [8] X. Wang, D. Vanderbilt, J. R. Yates, and I. Souza, *Phys. Rev. B* **76**, 195109 (2007).
- [9] J. Weischenberg, F. Freimuth, J. Sinova, S. Blügel, and Y. Mokrousov, *Phys. Rev. Lett.* **107**, 106601 (2011).
- [10] H.-R. Fu and G.-Y. Guo, *Phys. Rev. B* **84**, 144427 (2011).
- [11] M. Gradhand, D. V. Fedorov, P. Zahn, and I. Mertig, *Phys. Rev. Lett.* **104**, 186403 (2010).
- [12] S. Lowitzer, D. Ködderitzsch, and H. Ebert, *Phys. Rev. Lett.* **105**, 266604 (2010).
- [13] I. Turek, J. Kudrnovský, and V. Drchal, *Phys. Rev. B* **86**, 014405 (2012).
- [14] P. Štěpá, *J. Phys. C: Solid State Phys.* **15**, L717 (1982).
- [15] A. Crépeux and P. Bruno, *Phys. Rev. B* **64**, 014416 (2001).
- [16] F. D. M. Haldane, *Phys. Rev. Lett.* **93**, 206602 (2004).
- [17] T. Miyasato et al., *Phys. Rev. Lett.* **99**, 086602 (2007).
- [18] L. Ye, Y. Tian, X. Jin, and D. Xiao, *Phys. Rev. B* **85**, 220403 (2012).
- [19] Y. Shiomi, Y. Onose, and Y. Tokura, *Phys. Rev. B* **79**, 100404 (2009).

- [20] A. Shitade and N. Nagaosa, *J. Phys. Soc. Japan* **81**, 083704 (2012).
- [21] M. E. Rose, *Elementary Theory of Angular Momentum*, Wiley, New York, 1957.
- [22] M. E. Rose, *Relativistic Electron Theory*, Wiley, New York, 1961.
- [23] H. Eschrig, *The Fundamentals of Density Functional Theory*, B G Teubner Verlagsgesellschaft, Stuttgart, Leipzig, 1996.
- [24] N. A. Sinitsyn, A. H. MacDonald, T. Jungwirth, V. K. Dugaev, and J. Sinova, *Phys. Rev. B* **75**, 045315 (2007).
- [25] J. Minár et al., *Nucl. Inst. Meth. Phys. Res. A* **547**, 151 (2005).
- [26] J. Minár, *J. Phys.: Cond. Mat.* **23**, 253201 (2011).
- [27] H. Ebert, D. Ködderitzsch, and J. Minár, *Rep. Prog. Phys.* **74**, 096501 (2011).
- [28] H. Ebert, S. Mankovsky, D. Ködderitzsch, and P. J. Kelly, *Phys. Rev. Lett.* **107**, 066603 (2011).
- [29] E. M. Gololobov, E. L. Mager, Z. V. Mezhevich, and L. K. Pan, *phys. stat. sol. (b)* **119**, K139 (1983).
- [30] M. Büttiker, *Phys. Rev. Lett.* **57**, 1761 (1986).
- [31] J. Banhart, R. Bernstein, J. Voithländer, and P. Weinberger, *Solid State Commun.* **77**, 107 (1991).
- [32] J. Banhart, H. Ebert, P. Weinberger, and J. Voithländer, *Phys. Rev. B* **50**, 2104 (1994).
- [33] E. Roman, Y. Mokrousov, and I. Souza, *Phys. Rev. Lett.* **103**, 097203 (2009).
- [34] P. N. Dheer, *Phys. Rev.* **156**, 637 (1967).
- [35] J. M. Lavine, *Phys. Rev.* **123**, 1273 (1961).
- [36] The implementation of the LSDA+DMFT in the KKR framework is reviewed in [26]. The LSDA+ U is obtained by retaining the static part of the self-energy. Around mean field double counting corrections are employed. The values for U and J_{eff} are commonly used in the description of 3d-TM.
- [37] Note that in our previous calculation [12] we obtained for Ni a value of -1635 S/cm which deviates by 20% from the value reported here. This was due to an inappropriate small setting for the muffin-tin radii r_{MT} (i. e. no touching spheres) used in the calculations which employ the atomic-sphere approximation (ASA, r_{ASA}) for the potential construction. The muffin-tin zero in the KKR calculation is obtained by an averaging over the area between r_{MT} and r_{ASA} . For Ni it turns out that the AHC is very sensitive to such an inappropriate setting. We checked this issue for Fe and Co and found no such sensitivity, i. e. shrinking r_{MT} by 5% only changed the AHC values by at most 2%.
- [38] C. Y. Ho et al., *J. Phys. Chem. Ref. Data* **12**, 183 (1983).
- [39] S. Onoda, N. Sugimoto, and N. Nagaosa, *Phys. Rev. B* **77**, 165103 (2008).
- [40] S. Lowitzer et al., *Phys. Rev. Lett.* **106**, 056601 (2011).